

Measurement of Small Angle Fiber Misalignments in Continuous Fiber Composites

S. W. Yurgartis*

Materials Engineering Department, Rensselaer Polytechnic Institute,
Troy, NY 12180-3590 (USA)

(Received 11 May 1987; accepted 17 July 1987)

SUMMARY

In aligned, continuous fiber composites the fibers actually wander with small angular misalignments about the mean direction. These misalignments are suspected of having a significant influence on several mechanical properties, such as longitudinal compression strength and tensile modulus. A technique is presented for measuring the volume fraction distribution of fiber misalignment angle in the range of $\pm 10^\circ$, with an estimated resolution of $\pm 0.25^\circ$. The method can provide a full bivariate distribution, which includes both in-plane and out-of-plane misalignments. Data from a carbon fiber composite, APC-2, are given as an illustration. Misalignment distributions for prepreg, a 0/90 laminate, and a unidirectional laminate are given. It is found that the distribution in the prepreg is axially symmetric, but changes upon lamination, the changes depending on stacking sequence. In this particular material most of the fibers are found to lie within $\pm 3^\circ$ of the mean fiber direction. Distribution standard deviations range from 0.693 to 1.936 degrees.

1 INTRODUCTION

Continuous, non-woven fibers in high-performance composites, though all nominally aligned in the same direction within a ply, have in fact small angular misalignments about their mean direction. The origins of fiber misorientation are still a matter of speculation; Swift¹ lists several possible sources. Nonetheless, the presence of angular misalignment—sometimes referred to as fiber waviness—has been recognized for many years. Over this

* Present address: Department of Mechanical and Industrial Engineering, Clarkson University, Potsdam, NY 13676, USA.

period of time fiber misalignment has been suspected of having a significant influence on composite properties such as longitudinal tensile modulus,¹⁻⁸ longitudinal compression strength,⁹⁻¹⁴ transverse mechanical and transport properties,^{2,6-8} delamination fracture toughness, and laminate consolidation,¹⁵ among others.

The absence of a means of quantitatively measuring small angular misalignments has made these suspicions and resulting theories difficult to test. This paper describes a technique for measuring the distribution of fiber misalignments. The technique is particularly well suited to measuring small misalignments typically found in high-performance composites—misalignments in the range $-10^\circ < \phi < 10^\circ$.

To illustrate the method, misalignment distributions from a sample of APC-2, a carbon fiber/polyether etherketone composite material commercially available from ICI Ltd, are given. Data presented will show the initial misorientation distribution in the prepreg, and will also demonstrate how the final distribution is influenced by lamination and stacking sequence. Both in-plane and out-of-plane angle distributions are measured, and as will be shown these are marginal distributions which, taken together, give a good measure of the full three-dimensional misalignment distribution.

2 PREVIOUS WORK

Previous work to measure fiber angle has been primarily confined to short-fiber composites. Direct measurement with a protractor on micrographs or with an angular reticule in a microscope is typical.¹⁶⁻¹⁸ Most effort has gone into preparing suitable sample sections, such as sections with sufficient contrast between fiber and matrix. McGee and McCullough have developed an elegant diffraction technique to obtain a single parameter measure of short-fiber orientation.¹⁹ In continuous glass fiber composites, which are transparent in thin sections, colored tracer fibers have been used to observe fiber orientation, again by direct measurement.²⁰

These techniques appear to be limited to measuring quite large misorientations that occur during flow and forming operations. None seems applicable to, or to have sufficient resolution, for the measurement of small angular misalignments found in typical, unidirectional, continuous fiber composites. Though not reviewed in this paper, the strong predicted sensitivity of, for example, longitudinal compression strength on fiber misalignment (e.g. a change from 1° to 2° misalignment results in a 50% drop in strength⁹) makes a resolution of $\pm 0.5^\circ$ or better highly desirable. Also desirable is the ability to measure the complete misalignment distribution.

3 MEASURING FIBER MISALIGNMENT—2D CASE

For ease of illustration early discussion will be confined to the two-dimensional case. The technique is based on the simple observation that a plane section of a circular cylinder is an ellipse. The major axis of the ellipse, l , is related to the angle between the sectioning plane and the cylinder axis, ω (see Fig. 1), by

$$\sin \omega = \frac{d}{l} \quad (1)$$

where d is the cylinder diameter. If an array of cylinders were cut by the same plane, then measuring the distribution of l_i might give the distribution of ω_i , where the subscript indicates the i th cylinder.

To apply these observations to the determination of the fiber angle distribution in a composite, it must be assumed (1) that short sections of fibers are approximately straight and (2) that all fibers have the same circular diameter. Initially these assumptions are accepted: they are examined more closely below.

In practice the method requires several steps. The composite sample must be sectioned and polished, the distribution of l_i measured, and the distribution of ω_i calculated. A transformation is also needed from the angles ω_i to the angles ϕ_i , where ω_i is the angle that the i th fiber segment makes with respect to the sectioning plane and ϕ_i is the angle of this same fiber, but with respect to the mean fiber direction.

In principle the composite of interest can be sectioned at any plane-cut angle, ϕ_{PC} , as shown in Fig. 2. The mean fiber direction is defined as the 0°

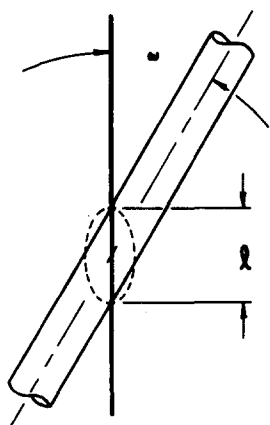


Fig. 1. Ellipse resulting from the plane section of a right circular cylinder.

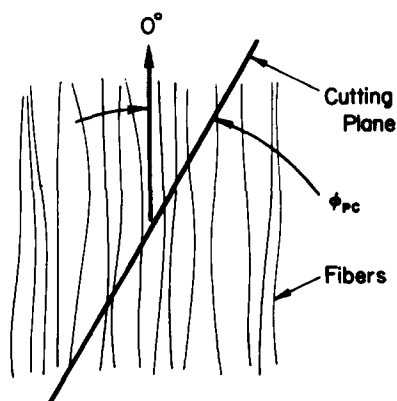


Fig. 2. Definition of the plane-cut angle ϕ_{PC} .

direction. A proper choice of ϕ_{PC} , however, is a key factor in the technique described here. An examination of eqn (1) and four considerations suggests a limited choice of ϕ_{PC} . First, the sensitivity of l to ω is greatest when ω is small, which leads to better angular resolution. Second, as ω approaches zero, l rapidly becomes large and thereby weakens the assumption that measured fiber segments are straight. It also makes these ellipse lengths experimentally difficult to measure. Third, as will be discussed below, the measured distribution folds back upon itself when $\omega < \phi_{PC}$. Finally, the calculated ω is less sensitive to variations in fiber diameter when ω is small.

Given these considerations a balanced choice for ϕ_{PC} must be made. For example, the illustrative data given later were measured at $\phi_{PC} \approx 5^\circ$. Therefore most of the fiber segments—the segments near the 0° direction—are at an angle of about 5° to the sectioning plane. The ellipse axis lengths, l_i , are then about 12 fiber diameters, and a 1° difference in ω will result in a 20% difference in l . The measurement of these dimensions with good accuracy has proved to be experimentally feasible. In other composites a different choice of ϕ_{PC} may be better suited to different circumstances. Different values of ϕ_{PC} can also be chosen for the same material to optimize different objectives. For example, a sample with a narrow angle distribution will have better measurement resolution if a smaller ϕ_{PC} is chosen.

4 CORRECTING FOR COUNTING BIAS

Transformation from a measured distribution of $f(l)$ to the distribution $f(\omega)$ is not as straightforward as it might appear. The objective is to obtain a measure of the proportion of the overall fiber volume fraction in a given volume of material that is at a local misalignment angle near ω_i . Consider a cubic volume element of composite material with a single fiber traversing the element, as shown in Fig. 3. A random plane section taken through this cube, parallel to the top face ($\omega_i = \text{constant}$), is more likely to intersect a fiber with large ω_i than with small ω_i . Thus, a count of the number of fibers with ellipse axis length l_i will be biased toward counting fibers at large ω_i (small l_i) more frequently than fibers with small ω_i . Fortunately this is a long-standing stereological problem, and it is possible to use the generally developed theory to derive a specific correction for the circumstances at hand.

Starting from the established stereological relationship,²¹

$$N_{A_i} = N_{V_i} D_{V_i}(\omega) \quad (2)$$

where N_{A_i} is the average number of objects of class i counted per unit area, N_{V_i} is the average number of class i objects per unit volume, and D_{V_i} is the

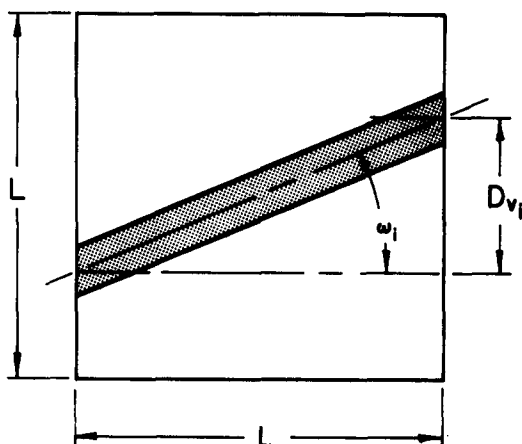


Fig. 3. A volume element of composite traversed by a single fiber; used to illustrate the counting bias correction.

distance between tangent planes of the i th class object (restricted to two dimensions). In this case simple geometry gives

$$D_{v_i} = L \tan \omega_i \quad (3)$$

By definition

$$N_{A_i} = \frac{N_i}{L_r W} \quad (4)$$

where L_r is the length of the measurement field, W is the width of the measurement field, and N_i is the number of fibers counted. Substituting into eqn (2) gives

$$N_{v_i} = \frac{N_i}{L_r W (L \tan \omega_i)} \quad (5)$$

The number fraction, on a volume basis, of fibers at angle ω_i is obtained simply as

$$f_N(\omega_i) = \frac{\frac{N_i}{L_r W (L \tan \omega_i)}}{\sum_1^n \frac{N_i}{L_r W (L \tan \omega_i)}} \quad (6)$$

which reduces to

$$f_N(\omega_i) = \frac{\frac{N_i}{\tan \omega_i}}{\sum_1^n \left(\frac{N_i}{\tan \omega_i} \right)} \quad (7)$$

Neglecting the small difference in fiber-segment volume when the fiber is at different angles within volume L^3 gives, to a good approximation,

$$f_V(\omega_i) = \frac{\frac{N_i}{\tan \omega_i}}{\sum_1^n \left(\frac{N_i}{\tan \omega_i} \right)} \quad (8)$$

where $f_V(\omega_i)$ is the volume fraction of the total volume of fiber that is at an angle ω_i to the plane-cut surface. Equation (8) is in terms of measurable quantities. (For convenience in notation the subscripts V and i will be dropped.)

While $f(\omega)$ is a continuous distribution in reality, in practice it is approximated by a discrete distribution similar to (8), where the range of angles is partitioned into intervals.

5 TRANSFORMATION OF THE DISTRIBUTION

Finally, it is necessary to transform from the angle ω , referenced to the sectioning plane, to the angle ϕ , referenced to the zero degree fiber direction. The transformation is simply

$$\phi = \omega - \phi_{PC} \quad (9)$$

Because ϕ_{PC} cannot be known with good accuracy *a priori*, it is determined from $f(\omega)$. Since the zero degree direction is the mean of the fiber misalignment distribution, the mean of $f(\omega)$ equals ϕ_{PC} . Thus, $f(\phi) = f(\omega - \bar{\omega})$.

Two factors which may distort the estimated distribution $f(\phi)$ must be noted. Both factors also affect the equality $\bar{\omega} = \phi_{PC}$, and therefore the discussion will be in terms of the untransformed distribution $f(\omega)$. First, fiber segments with $\omega \approx 0$ will be unlikely to be properly measured because l will be large. Thus, these fibers may not be counted at all if l exceeds the measurement field boundaries or, more likely, because of fiber curvature these fibers will be counted as having angles somewhat larger than they actually have. In other words, these fibers will be less likely to conform to the first basic assumption noted earlier in this paper, i.e. measured fiber segments are straight. The second distorting factor is that fiber segments at an angle $\omega_i < 0$ will be measured as fibers with a positive ω_i , probably in the low angle part of the $f(\omega)$ distribution. The distribution at $\omega_i < 0$ folds back upon itself.

It is possible to estimate the magnitude of these distortions by making the reasonable assumption that the true fiber angle distribution is symmetric.

The distortion due to folding can then be judged by looking at the upper end of the $f(\omega)$ distribution where $\omega_i > 2\bar{\omega}$. Distortion due to miscounting of fibers at $\omega_i \approx 0$ can also be estimated from the non-symmetry of the measured distribution.

In practice—specifically in the examples given below—these distortions are not seen to be a problem. Again, careful choice of ϕ_{PC} can minimize errors. In cases where the distortions are judged substantial it is usually possible to circumvent them. Recognizing that the distortions occur primarily at the lower end of the $f(\omega)$ distribution, and accepting the assumption of a symmetric distribution, the lower portion of the distribution can be discarded and the upper ‘half’ used to estimate the distribution $f(\phi)$. The transformation from $f(\omega)$ to $f(\phi)$ cannot now be based on $\phi_{PC} = \bar{\omega}$, since the distribution of ω is distorted. Instead ϕ_{PC} is accurately given by the mode of $f(\omega)$, although the median of $f(\omega)$ will be almost an equally good measure of ϕ_{PC} and is more accurately obtained from the data. In short, $f(\phi)$ is based on the measured distribution $f(\omega)$ at $\omega \geq \omega_{\text{median}}$, with the transformation $\phi = \omega - \omega_{\text{median}}$. The cost is in discarding data, most of which is accurate, and also possibly reduced angular resolution due to reduced sensitivity at larger angles, as mentioned previously.

6 GENERALIZATION TO THREE DIMENSIONS

Real composites will of course have fibers misaligned in three dimensions, as shown in Fig. 4. Using the natural geometry of typically planar composite structures, it is convenient to think of fiber misalignment occurring both (a) in the plane of the laminate and (b) out of the plane of the laminate. The

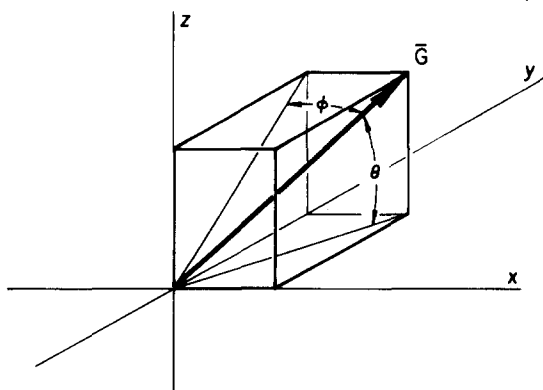


Fig. 4. Definition of the in-plane and out-of-plane misalignment angles, ϕ and θ , respectively. The fiber axis is represented by vector \vec{G} .

question that arises is: how will the two-dimensional analysis given above be affected by fibers that are really three-dimensionally misaligned?

Consider a circular cylinder—representing a fiber—in a right-handed XYZ coordinate system. The cylinder axis direction is given by the unit vector

$$\vec{G} = (a_1, a_2, a_3)$$

where a_i are the direction cosines. The equation of the cylinder can be shown to be

$$X^2(1 - a_1^2) + Y^2(1 - a_2^2) + Z^2(1 - a_3^2) - 2YXa_1a_2 - 2XZa_1a_3 - 2ZYa_2a_3 = r^2 \quad (10)$$

where r is the radius. The plane section which results from the intersection of the plane $X=0$ and the cylinder described by \vec{G} is

$$Y^2(1 - a_2^2) - 2ZYa_2a_3 + Z^2(1 - a_3^2) = r^2 \quad (11)$$

which is readily verified to be the equation of an ellipse. Here the plane $X=0$ is equivalent to the sectioning plane mentioned earlier, and the major axis of the ellipse is the quantity previously termed l .

Taking the plane of a flat laminated composite as the X - Y plane, eqn (11) can be written in terms of in-plane misalignment angle, ϕ , and out-of-plane misalignment angle, θ (see Fig. 4), by recognizing that

$$\sin \theta = a_3 \quad \sin \phi = a_1$$

and

$$a_1^2 + a_2^2 + a_3^2 = 1$$

Thus, sectioning by the plane $X=0$ of a fiber that is misaligned in the direction given by θ and ϕ results in the ellipse

$$Y^2(\sin^2 \phi + \sin^2 \theta) - 2ZY(1 - \sin^2 \phi - \sin^2 \theta)^{1/2}(\sin \theta) + Z^2(1 - \sin^2 \theta) = r^2 \quad (12)$$

The major axis diameter, l , can be determined by standard analytic geometry.²²

The sensitivity of measured in-plane misalignment, ϕ , to a simultaneous out-of-plane misalignment, θ , can now be determined. The result, as might be anticipated from careful inspection of Fig. 4, is that the major axis diameter, l , at any given angle, ϕ , is independent of the angle, θ . Using the same considerations it is also apparent that θ could be measured independently of ϕ .

The independence between ϕ and θ can be used to good advantage. Both the distributions $f(\phi)$ and $f(\theta)$ can be determined independently. To measure $f(\phi)$ the plane-cut section is made by a plane normal to the plane of the

laminate. The analysis remains the same as given above for the two-dimensional case. To measure $f(\theta)$ the sectioning plane is approximately orthogonal to the $f(\phi)$ sectioning plane and is almost in the plane of the laminate. The analysis proceeds identically.

The distributions $f(\phi)$ and $f(\theta)$ are so-called marginal distributions of the total bivariate, three-dimensional angle distribution, $f(\phi, \theta)$. If it is assumed that fiber segment misalignments are statistically independent—in other words, there is no correlation between θ and ϕ —then

$$f(\phi, \theta) = f(\phi)f(\theta) \quad (13)$$

7 EXPERIMENTAL MEASUREMENTS

Data on fiber angle distribution in APC-2 composite material illustrate the measurement technique and provide data of interest in themselves. APC-2 material was chosen because it was readily available in our laboratory. Its appearance is similar to other high quality preregs.

The fundamental measured quantity is l_i . In this work l_i is measured from micrographs using a digitizing table interfaced to a microcomputer. Micrographs are prepared by first potting a sample in epoxy resin. The potted sample is accurately sectioned flat with a swing-grinder at an estimation of ϕ_{PC} . After careful metallographic polishing the section is photographed with reflected light microscopy; Fig. 5 is a portion of a micrograph. A photograph is taken of a stage micrometer and prepared in parallel with the sample micrographs. Magnification choice is based on a practical estimate of how accurately length data can be obtained from the digitizing table. In this case a resolution of ± 0.5 mm proved feasible, so a magnification which resulted in l (at $\omega = 5^\circ$) of about 20 mm was chosen, giving a resolution of $\pm 2.5\%$ (which translates into an angular resolution of about $\pm 2.5\%$).

At this magnification (about 245:1 on the micrograph) it is not possible to measure the fiber diameter of each fiber with sufficient resolution. Therefore a separate measurement of fiber diameter was made: Fig. 6 shows the diameter distribution as measured with a Ziess IBAS image analyzer on a high magnification section taken transverse to the fiber axes. These XAS fibers have a fairly narrow diameter distribution with mean, $\bar{d} = 6.93 \mu\text{m}$, and standard deviation of $0.31 \mu\text{m}$. In addition, the assumption of circular cross-section, as checked with a circle template, appears to be very good.

A simple microcomputer program takes the l_i data and calculates ω_i using eqn (1) with the mean fiber diameter. About 800 or more ellipse lengths are measured for each distribution calculation. The ω_i are sorted into bins of width half a degree. The width of the bins is not critical, but the choice made

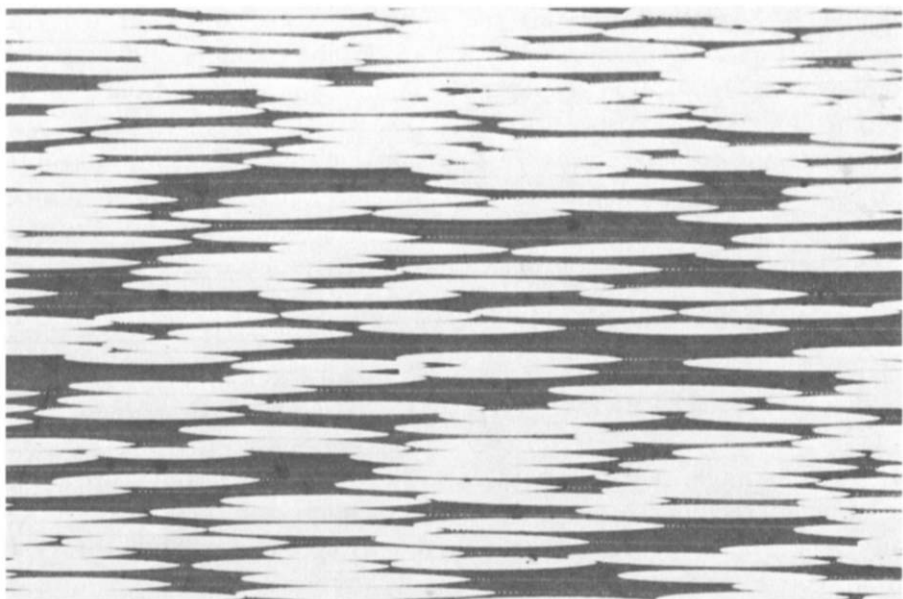


Fig. 5. Example of a micrograph used to obtain ellipse length data; only a portion of the micrograph is shown.

here is motivated by recognizing that at $\omega \approx 5^\circ$ an uncertainty in fiber diameter of ± 1 standard deviation results in an angular uncertainty of about $\pm 0.24^\circ$. The program then calculates eqn (8) and presents the results as a histogram. The average angle, $\bar{\omega}$, is also calculated on the basis of histogram data, which have now been corrected for the sample counting bias described earlier. Finally, the transformation between ω and ϕ is made, in

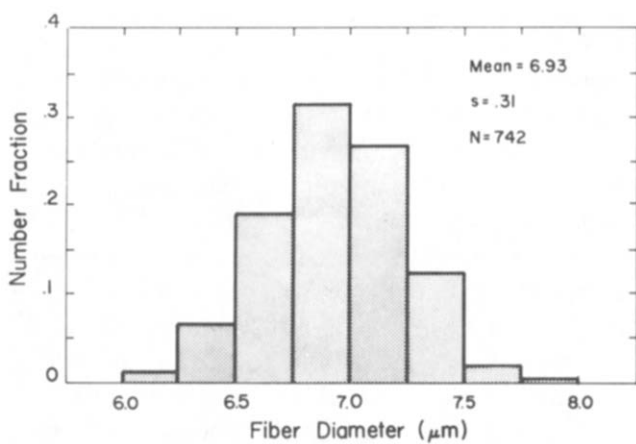


Fig. 6. XAS carbon fiber diameter distribution.

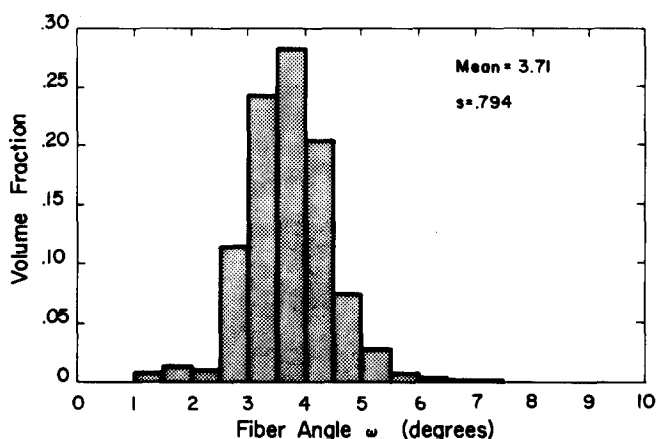


Fig. 7. Untransformed fiber angle distribution; from in-plane APC-2 prepreg.

this case using eqn (9) and assuming uniform distribution across each bin width. The distribution standard deviation, s , is also calculated.

Figure 7 shows the distribution, in terms of ω , of the in-plane fiber misalignment in APC-2 prepreg. Notice that the distribution is reasonably symmetric about the mean. The data shown in Fig. 7 can be used to estimate the validity of the two basic assumptions noted earlier—that is, measured fiber segments are straight and fiber diameter is constant. An estimate of sensitivity to fiber diameter is obtained by recalculating the data in Fig. 7 based on different fiber diameters. For $d = 6.62 \mu\text{m}$, $\bar{\omega} = 3.54^\circ$ and $s = 0.814^\circ$. For $d = 7.24 \mu\text{m}$, $\bar{\omega} = 3.88^\circ$ and $s = 0.767^\circ$. Thus, loosely estimated, the standard deviation of the measured distribution has an uncertainty of about $\pm 0.04^\circ$. Estimating how well the assumption of straight fiber segments holds is less easy. Physically it seems reasonable to treat fiber segments of roughly 20 fiber diameter lengths as straight, and the micrographs do not indicate otherwise. Also the symmetry of the $f(\omega)$ distributions implies that the assumption is reasonable.

Returning to the data in their final form, Fig. 8 plots both in-plane and out-of-plane distributions of the prepreg transformed about a mean of zero. Two observations are notable. First, the distribution is quite narrow—83% of the fiber volume is within $\pm 1^\circ$ of being perfectly aligned. Second, the in-plane and out-of-plane distributions are, perhaps unexpectedly, axially symmetric. This may be an important clue about the original source of fiber misalignment in the prepreg.

When eight plies of prepreg are laminated together (using standard procedures, 380°C , 100 psi, 10 min), the distributions are found to change. It should be noted that all samples are from a continuous length of prepreg less than 2 m long. In Fig. 9, the in-plane distributions are shown for (a) the

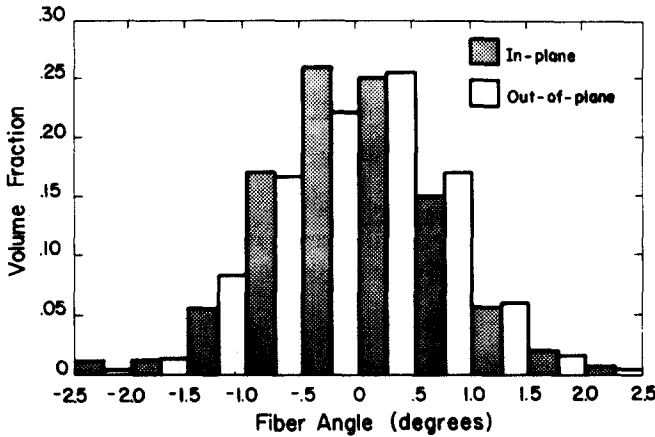


Fig. 8. In-plane and out-of-plane fiber misalignment distributions from APC-2 prepreg. Sample sizes 781 and 1111, respectively.

prepreg, (b) the third ply of a $(0/90)_{2s}$ laminate, and (c) a unidirectional laminate. The same sequence, but for out-of-plane misalignment, is shown in Fig. 10. In-plane alignment is seen to deteriorate in the same relative order, becoming quite broad for the unidirectional laminate. The unidirectional in-plane sample showed a weak grouping among fibers of about the same misorientation. This grouping appears to be due to a cooperative waviness among bundles of fibers: the distribution in Fig. 9 reflects this behavior. Out-of-plane alignment may slightly improve for the 0/90 laminate. The perpendicular fibers in the lamina above and below the third ply presumably help straighten the fibers. Out-of-plane alignment in the unidirectional laminate worsens, but not as much as the in-plane alignment.

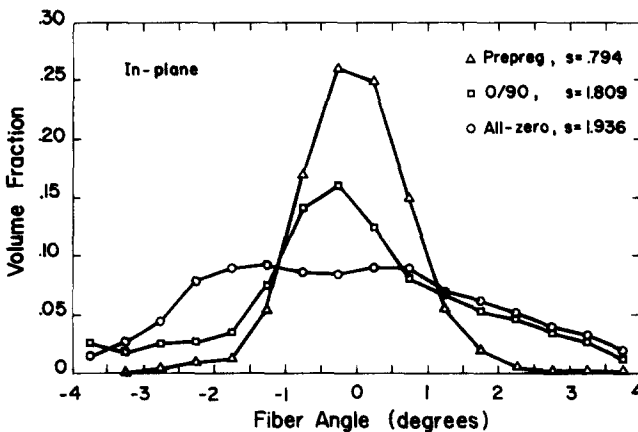


Fig. 9. In-plane misalignment for prepreg, a 0/90 laminate, and all-zero laminate. Sample sizes 781, 1036 and 2143, respectively.

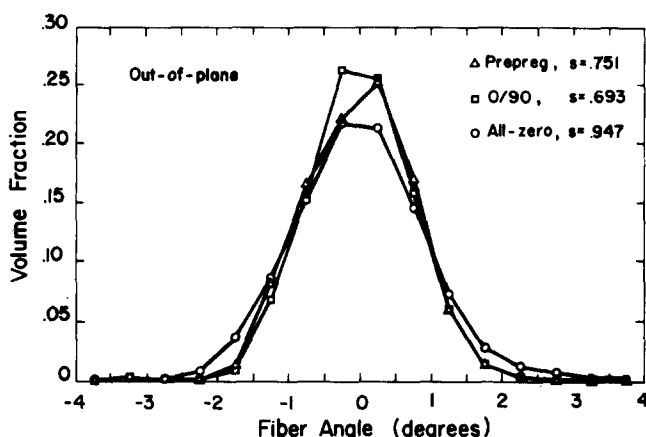


Fig. 10. Out-of-plane misalignment for prepreg, a 0/90 laminate, and all-zero laminate. Sample sizes 1111, 1133 and 1044, respectively.

The data given above demonstrate that lamination can change the fiber misalignment distribution: not only can $f(\phi)$ narrow or broaden, but it can also become axially non-symmetric. It seems reasonable to suspect that changes in lamination procedure, or different resin flow fields found in different composite systems, could lead to changes in the distributions, and ultimately differences in mechanical properties.

A normal distribution fits the measured distributions moderately well. For example, using the third ply 0/90 data leads to the bivariate normal distribution:

$$f'(\phi, \theta) = 0.101 \exp \left[-\frac{1}{2} \left(\frac{\phi^2}{3.27} + \frac{\theta^2}{0.48} \right) \right]$$

8 DISCUSSION

The technique presented here for making fiber angle misalignment measurements appears to have sufficient resolution to be useful. The largest uncertainty results from the distribution of fiber diameters. An analysis which explicitly incorporates fiber diameter variation into the fiber angle statistics could probably be developed. In many cases, though, it may be unnecessary. Additionally, newer carbon fibers made with refined process controls appear to have narrower diameter distributions, though data are scarce. Errors can also arise as a result of polishing artifacts, and care must be taken to avoid significant damage to the fiber edges. Manual collection of data, such as used to acquire the data given above, is a fairly long process, and automation of the l_i measurements with an image analysis machine is

attractive. It should also be noted that although the fiber angle distribution can be determined, the shape of the fiber curvature is still unknown; this would be useful information and deserves future study. More work is also needed in fitting statistical models to the data.

The technique may prove useful in peripheral applications. Consistency of alignment between plies that are ostensibly stacked in the same orientation could be very accurately checked. In tests where fiber alignment relative to the sample geometry is critical, the technique could be used to determine precisely the mean fiber direction in the test plaque. Fiber misalignment may also be an unrecognized but significant issue in prepreg quality control. Variations in misalignment distribution from run-to-run or even within a run may help explain scatter in mechanical property measurements.

The misalignments shown in Figs 8–10, though small, are of a magnitude to be relevant to most of the structure–property theories referenced earlier. It is not yet known if these distributions are typical of this class of composite, but they do suggest the magnitude of misalignment to be found in similar materials.

A fundamental question remains unanswered. How are fiber misalignment distributions related to composite mechanical and transport properties? Existing theories need more testing, and will probably need to be expanded to incorporate the statistical nature of fiber misalignment. The ability to measure fiber misalignment opens many possibilities for experiments seeking to establish a connection between microstructure and properties.

ACKNOWLEDGEMENTS

Dr Michael Vallance, General Electric Research and Development, very kindly provided the fiber diameter measurements. The APC-2 material was generously supplied by Dr Roy Moore, ICI Ltd. Both Dr Steven J. Winckler and Mr Krishna Shrinivasan provided useful comments on the draft manuscript.

REFERENCES

1. D. G. Swift, Elastic moduli of fibrous composites containing misaligned fibres, *J. Phys. D: Appl. Phys.*, **8** (1975) p. 223.
2. V. V. Bolotin, Theory of a reinforced layered medium with random initial irregularities (Engl. trans.), *Polym. Mechanics*, **2** (1966) p. 7.
3. Yu. M. Tarnopol'skii, G. G. Portnov and I. G. Zhigun, Effect of fiber curvature

- on the modulus of elasticity for unidirectional glass-reinforced plastics in tension (Engl. trans.), *Polym. Mechanics*, **3** (1967) p. 161.
4. A. V. Nosarev, Effect of curvature of the fibers on the elastic properties of unidirectionally reinforced plastics (Engl. trans.), *Polym. Mechanics*, **3** (1967) p. 567.
 5. J. Cook, The elastic constants of an isotropic matrix reinforced with imperfectly oriented fibres, *Brit. J. Appl. Phys.*, **2** (1968) p. 799.
 6. R. H. Knibbs and J. B. Morris, The effect of fibre orientation on the physical properties of composites, *Composites*, **5** (1974) p. 209.
 7. W. H. M. van Dreumel and J. L. M. Kamp, Non-Hookean behavior in the fibre direction of carbon-fibre composites and the influence of fibre waviness on the tensile properties, *J. Comp. Mat.*, **11** (1977) p. 461.
 8. J. Jortner, A model for predicting thermal and elastic constants of wrinkled regions in composite materials, in *Effects of Defects in Composite Materials*, ASTM STP 836, 1984, pp. 217–36.
 9. A. S. Argon, Fracture of composites, in *Treatise on Materials Science and Technology* (ed. H. Herman), Vol. 1, Academic Press, New York, 1972, pp. 78–114.
 10. G. M. Martinez, M. R. Piggott, D. M. R. Bainbridge and B. Harris, The compression strength of composites with kinked, misaligned, and poorly adhering fibres, *J. Mat. Sci.*, **16** (1981) p. 2831.
 11. M. R. Piggott, A theoretical framework for the compressive properties of aligned fibre composites, *J. Mat. Sci.*, **16** (1981) p. 2837.
 12. A. S. Wronski and T. V. Parry, Compressive failure and kinking in uniaxially aligned glass-resin composite under superposed hydrostatic pressure, *J. Mat. Sci.*, **17** (1982) p. 3656.
 13. B. Budiansky, *Micromechanics, Computers and Structures*, **16** (1983) p. 3.
 14. H. T. Hahn and J. G. Williams, Compression failure mechanisms in unidirectional composites, *NASA Tech. Memo.* 85834 (1984).
 15. T. G. Gutowski, Z. Cao, J. Kingery and S. J. Wineman, Resin flow/fiber deformation experiments, *SAMPE Quarterly*, **17** (1986) p. 54.
 16. S. R. Doshi, J. M. Dealy and J. M. Charrier, Flow induced fiber orientation in an expanding channel tubing die, *Polym. Eng. Sci.*, **26** (1986) p. 468.
 17. M. Vincent and J. F. Agassant, Experimental study and calculations of short glass fiber orientation in a center gated molded disc, *Polym. Composites*, **7** (1986) p. 76.
 18. M. R. Kamal, L. Song and P. Singh, Measurement of fiber and matrix orientations in fiber reinforced composites, *Polym. Composites*, **7** (1986) p. 323.
 19. S. H. McGee and R. L. McCullough, Characterization of fiber orientation in short-fiber composites, *J. Appl. Phys.*, **55** (1984) p. 1394.
 20. P. K. Mallick, Effect of fiber misorientation on the tensile strength of compression molded continuous fiber composites, *Polym. Composites*, **7** (1986) p. 14.
 21. R. T. DeHoff and E. N. Rhines, *Quantitative Microscopy*, McGraw-Hill Co., New York, 1968, pp. 129–32.
 22. E. S. Smith, M. Salkover and H. K. Justice, *Analytic Geometry*, 2nd edn, John Wiley & Sons, New York, 1954.